Hindawi
International Journal of Antennas and Propagation
Volume 2024, Article ID 1861253, 10 pages
https://doi.org/10.1155/2024/1861253

Research Article

On Design and Verification of an Efficient Microwave Wireless Power Transmission System

Baoxian Zheng,[1] Kunding Ma,[2] Yuanyuan Liu,[2] Tong Jiang,[2] Tingyi Liu,[3] Qishuai Ma,[3] Yi Liu,[4] Lin Yang,[5] and Xi Li[5]

[1]*Aerospace Times FeiHong Technology Company Limited, Beijing 100094, China*
[2]*China Academy of Space Technology (Xi'an), Xi'an 710100, Shaanxi, China*
[3]*Shaanxi University of Technology, Hanzhong 710071, Shaanxi, China*
[4]*The 39th Research Institute of China Electronics Technology Group Corporation, Beijing, China*
[5]*Xidian University, Xi'an 710071, Shaanxi, China*

Correspondence should be addressed to Xi Li; xli@xidian.edu.cn

Received 15 December 2023; Revised 23 January 2024; Accepted 31 March 2024; Published 23 April 2024

Academic Editor: Giuseppina Monti

We report on the theoretical design and experimental verification of a high efficiency microwave wireless power transmission (MWPT) system operating in the Fresnel region. To achieve high conversion efficiency over a transmit distance of 11 meters, the transmit reflector antenna was optimized to locate the focal point at 11 m. The size of the receive antenna was decided by calculating the field distribution and the received power at different positions in the receive antenna aperture. Furthermore, an accurate model of the diode is presented, which was imported into the ADS software for high-precision rectifying circuit design. As a result, an overall DC-DC conversion efficiency of 20% was achieved, as measured in an anechoic chamber at a given distance of 11 m. The experimental results validated the proposed method.

1. Introduction

Microwave wireless power transmission (MWPT) has attracted increasing attention, owing to its capability of charging mobile phones and laptops, electric vehicles, and unmanned aerial vehicles (UAV) [1]. Moreover, it is one of the key technologies to realize space solar power satellites (SSPS). MWPT technologies can be broadly divided into radiative and nonradiative power transfer methods. As for the former, if the distance between transmit and receive antenna satisfying far-field (FF) condition long range MWPT can be achieved by means of microwave or laser sources [2, 3]. However, the achievable radiative power transmission efficiency in the FF region is often unacceptably low, mainly because of the size limitation of transmit and receive antennas. Nonradiative power transfer methods mainly include near-field magneto-inductive coupling [4] and Fresnel fields [5]. Systems operating in the reactive near-field zone can achieve high conversion efficiency since power is transferred between resonant circuits via magneto-inductive coupling. However, their efficiency decrease as $1 = d6$ [6], where d is the distance between transmit and receive antennas. In the Fresnel region, the Friis transmission equation is invalid since the FF pattern is not formed. In this case, the power transmission efficiency can be improved by focusing the field intensity from the source, and therefore, increasing the amount of power received by a receive antenna aperture placed at the focal point power received by a receiving antenna aperture placed at the focal point.

It is worth noting that in many applications, such as mobile devices, Internet of things, and sensors, do not require a long power transfer distance, but only a few meters, typically around 10 m [7]. In this case, to increase the power transmission efficiency, the aperture of the transmit antenna should be enlarged in order to narrow the beamwidth. The receive antenna is placed in the Fresnel zone rather than in the far-field region, at a mid-range of several meters. In

recent years, MWPT systems and methods operating in the Fresnel field have gained much attention due to their good conversion efficiency, medium-range distance, and acceptable antenna size [8–12]. In [8], the influence of the beam focus, and the taper distribution of the radiating field in the Fresnel zone have been discussed. In [9, 10], the designs of Fresnel MWPT systems which can achieve 66.5% and 33.2% RF-DC efficiency, respectively, have been reported. However, in both cases, the operating distance is only about 10λ, and the feeding network is complicated and easy to make systems defocus for a larger array. In [11], an MWPT system equipped with an optimal number of rectenna array elements for mid-range application and a parallel DC combing circuit is designed to improve conversion efficiency. Nevertheless, only a 5.01% RF-DC efficiency can be achieved at a distance of 1 m. Based on Bezier curves [12], a method for antenna aperture illumination design for MWPT in the Fresnel zone is reported in [13]. As a result, a larger aperture power coefficient can be achieved, with a slight reduction of the beam collection efficiency [14]. Publication [15] reports a compact, polarization-insensitive rectenna based on metasurface at a frequency of 5.8 GHz, it can reach the maximum conversion efficiency measured 66% under a 500 Ω load. Article [16] proposes a highly integrated multipolarization wideband rectenna for simultaneous wireless information and power transfer, the wireless power receiving port has conversion efficiency up to 76.5%.

In this paper, a new design of MWPT system operating in the Fresnel zone is presented. The main features of the proposed MWTP system can be summarized as follows: (i) a reflector antenna is deployed as the transmit antenna, which can enjoy advantages of low cost and no feeding network; (ii) an air-supported microstrip antenna is used as the receive antenna to reduce substrate loss; (iii) two-element series fed and four-element cascaded arrays are introduced such that different power densities can be adapted; (ii) and (iii) have been introduced in article [17]; (iv) a diode model is implemented to get its optimal characteristic and parameters, and a high-precision rectifying circuit model is designed accordingly; and (v) a parallel DC combing circuit is designed. By means of the proposed design, the resulting experimental conversion efficiency is 20%, as measured in an anechoic chamber at a distance of 11 m.

2. MWPT System Design

Figure 1 illustrates a schematic diagram of the MWPT system. It mainly includes microwave transmitter, transmit antenna, the receive antenna, rectifying, and the DC combiner circuits. It is known that the overall efficiency of the system relates to each of the aforementioned components. Thus, each component of the MWPT system should be carefully designed, and we shall discuss this in the sequal.

2.1. The Microwave Transmitter. In the MWPT system, the DC energy should be first converted to RF power, which is then radiated to the free space by the transmit antenna. In our designed system, a GaN power amplifier is introduced to achieve high output power, as illustrated in Figure 2. The maximum DC-RF conversion efficiency is 59.3% when the input power is 88 W.

2.2. Transmit Antenna Design. Since high DC-DC conversion efficiency is a primary objective for our MWPT system, a narrow beam width of the transmit antenna is expected. It is known that antenna array can be employed for this purpose. However, in our design, a reflector antenna was selected because of its low cost and no feeding network. In our design, the distance between the transmit antenna and the receive antenna is fixed at 11 meters.

Since the position of the focus is dependent on the antenna dimension, the size of the reflector antenna should be determined. To this end, we first give the power density $S(\rho)$ of the reflector antenna as

$$S(\rho) = \frac{1}{\eta} \cdot |E(\rho)|^2, \tag{1}$$

where η is the wave impedance and in free space we have $\eta = 120\pi$, ρ indicates the distance between the field point and the center in the transmit antenna aperture, and $|E(\rho)|$ means the electric field strength. Figure 3 shows a diagrammatic sketch relevant to these parameters. The total energy within the antenna aperture can be expressed as

$$\int_0^{D/2} \int_0^{2\pi} S(\rho)\rho d\rho d\varphi = P_t \cdot \eta_a, \tag{2}$$

where D denotes the diameter of the reflector antenna, P_t is the transmit power, and η_a is the antenna efficiency excluding leakage. In our design, a −10 dB aperture field distribution of the reflector is assumed. Letting $\eta = 120\pi$ and substituting (1) into (2), one obtains

$$\int_0^{D/2} |E(\rho)|^2 \rho d\rho = 60 \cdot P_t \cdot \eta_a. \tag{3}$$

The field in the axial direction $E(z)$ can be obtained by integrating the $|E(\rho)|$ field distribution at z position according to the following equation (5):

$$E(z) = A_0 \int_0^{2\pi} \int_0^{D/2} |E(\rho)| \frac{e^{-jk\sqrt{z^2+\rho^2}}}{\sqrt{z^2+\rho^2}} \rho d\rho d\varphi, \tag{4}$$

where z is the distance from the reflector antenna in the axial direction. Figure 4 displays the distribution of the normalized electric field along z, for different reflector antenna diameters $D = 2.0$ m, $D = 2.4$ m, and $D = 2.8$ m. As it can be observed in the figure, the electric field focuses at 11 m when $D = 2.4$ m. The transmit antenna size is therefore selected as 2.4 m in the designed WPT system.

2.3. Design of the Receiving Antenna. A low profile air-supported microstrip antenna is chosen as the receiving antenna element in order to reduce substrate loss and withstand high power. Moreover, two-element

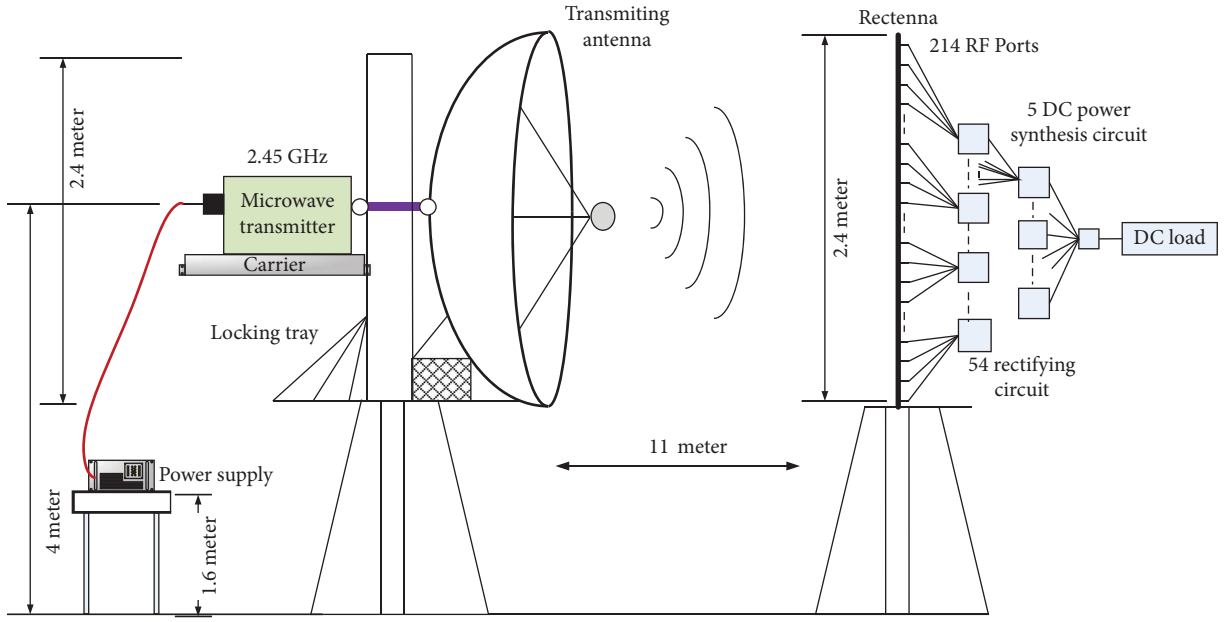

Figure 1: Schematic representation of the demonstrating MWPT system.

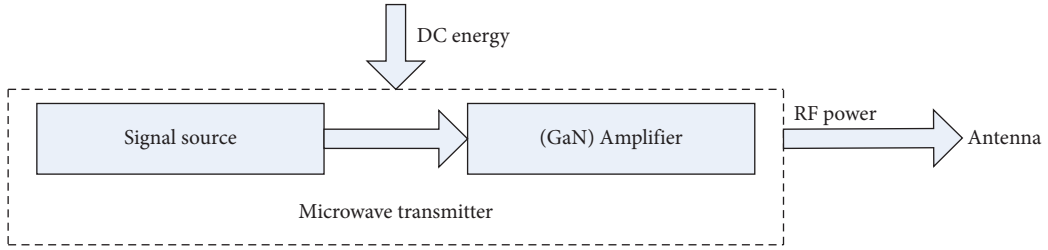

Figure 2: Sketch of the basic structure of the microwave transmitter.

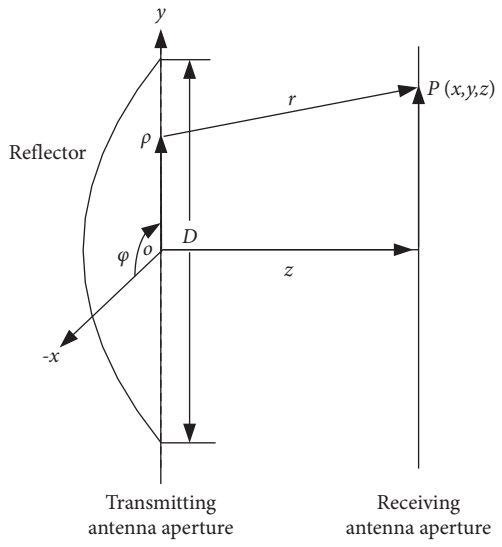

Figure 3: Diagrammatic sketch of proposed parameters relevant to the calculation of transmitting antenna size.

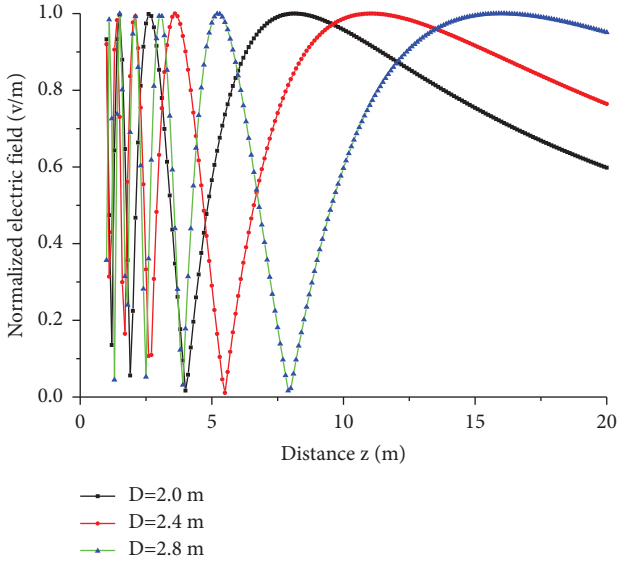

Figure 4: The normalized electric field along the axial direction z for different reflector antenna diameters.

series-fed and four-element cascaded arrays are introduced in order to adapt different power densities. This section was also introduced in the previous article [17].

The comparative results among antenna element, two-element series-fed array, and four-element cascaded array are presented in Table 1.

Table 1: Comparison among antenna parameters for the evaluated receiving antenna designs.

Receiving antenna	S_{11} (<−10 dB) (%)	E/H beamwidth at 2.45 GHz (°)	Gain at 2.45 GHz (dBi)
Element	4.1	53/63	8.6
Two-element	3.7	31/62	11.6
Four-element	4	31/39	13.5

2.4. Calculation of Received Power. The Friis transmission equations are not suitable for computing the RF power captured by the receiving antenna because the distance between the transmitting and the receiving antenna does not satisfy the FF condition. The received RF power can be computed by

$$P_r(x, y) = A_e(x, y) \cdot p(x, y), \tag{5}$$

where $P_r(x, y)$ denotes the power received by the antenna, whose effective receiving area is $A_e(x, y)$ at position (x, y), and $p(x, y)$ is the power density at position (x, y). $p(x, y)$ can be expressed as follows:

$$p(x, y) = p_m \cdot a(x, y), \tag{6}$$

where p_m is the maximum power density, and $a(x, y)$ is the normalized relative power density distribution. Finally, the following equation can be formulated:

$$P_r(x, y) = A_e(x, y) \cdot p_m \cdot a(x, y). \tag{7}$$

According to equation (3), we can write

$$\begin{aligned} P_t \cdot \eta_{tr} &= \int_{-\infty}^{\infty} \int_{-\infty}^{\infty} p(x, y) dx dy \\ &= p_m \cdot \int_{-\infty}^{\infty} \int_{-\infty}^{\infty} a(x, y) dx dy, \end{aligned} \tag{8}$$

where η_{tr} is the transmission efficiency between the transmitting antenna and the receiving antenna, including cable loss, coaxial connector loss, space transmission loss, polarization mismatch, field mismatch, and so on. Therefore, p_m can be expressed as

$$p_m = \frac{P_t \cdot \eta_{tr}}{\int_{-\infty}^{\infty} \int_{-\infty}^{\infty} a(x, y) dx dy}. \tag{9}$$

$P_r(x, y)$ can be reformulated as

$$P_r(x, y) = \frac{P_t \cdot \eta_{tr}}{\int_{-\infty}^{\infty} \int_{-\infty}^{\infty} a(x, y) dx dy} \cdot A_e(x, y) \cdot a(x, y), \tag{10}$$

and $a(x, y)$ can be computed by

$$a(x, y) = \frac{\int_0^{2\pi} \int_0^{\rho} |E(\rho)| \left(e^{-jkr}/r\right) d\rho d\varphi}{\left(\int_0^{2\pi} \int_0^{\rho} |E(\rho)| \left(e^{-jkr}/r\right) d\rho d\varphi\right)_{max}}, \tag{11}$$

$$r = \sqrt{(\rho \cos\varphi - x)^2 + (\rho \sin\varphi - y)^2 + z^2}, \tag{12}$$

where ρ is the distance between the field point and the center in the transmitting antenna aperture (see equation (1)), (x, y, z) means the position in the receiving antenna aperture, and r is the distance between the source point and the field point. According to equation (10), if the transmitted power P_t, the normalized relative power density distribution at a fixed distance from the transmitting antenna $a(x, y)$, and the effective receiving area $A_e(x, y)$ at position (x, y) are given, the received power can be computed. Figure 5 shows the normalized near field amplitude distribution at center row and at center column, at a distance of 11 m ($z = 11$ m in equation (12)) from the transmitting antenna. The size of the plotted near field area is 3 m × 3 m. A −10 dB aperture field distribution of the reflector is assumed for computations. As it can be seen from the plots, the field strength at a distance of 1.2 m from the center is about −10 dB, so the size of the receiving antenna is selected as 2.4 m.

It is worth to point out that since the rectifying efficiency is related to the input power to the rectifying circuit, input power should be kept as stable as possible. The gain of the antenna element can be related to the effective receiving area A_e by the following equation:

$$G = \frac{4\pi}{\lambda^2} \cdot A_e. \tag{13}$$

The computed gain of the simulated antenna element is 8.6 dBi, as obtained by HFSS software, so A_e can be calculated as 0.0086 m^2 according to equation (13). Substituting $A_e = 0.0086$ m^2, $P_t = 50$ W, and $\eta_{tr} = 0.5$ into equation (10), the distribution of P_r can be obtained (see Figure 6). The maximum received power by the antenna element is 22.6 dBm. Within the receiving area, a single antenna element is conveniently adopted where P_r is between 20 dBm and 22.6 dBm; two-element series-fed antenna array is a better choice where P_r is between 17 dBm and 20 dBm; four-element cascaded array is adopted where P_r is between 10 dBm and 17 dBm; the place is vacant where P_r is less than 10 dBm. According to this idea, the schematic view of the resulting antenna placement is shown in Figure 7. Green, red, and blue portions, respectively, indicate the single antenna elements, the two-element series-fed antenna arrays, and the four-element cascaded antenna arrays, each of them being connected to a single rectifying circuit. As a result, there are a total of 214 RF ports.

2.5. Rectifying Circuit Design. In a MWPT system, the rectifying circuit is one of the crucial components since the overall system efficiency mainly depends on the characteristics of the rectifying circuit [18]. An accurate model of the rectifying circuit is therefore mandatory. The accuracy of the model is mainly determined by the parameter acquisition of the diode, since other passive parts of the circuit can be easily modeled and simulated. Therefore, the diode model is of

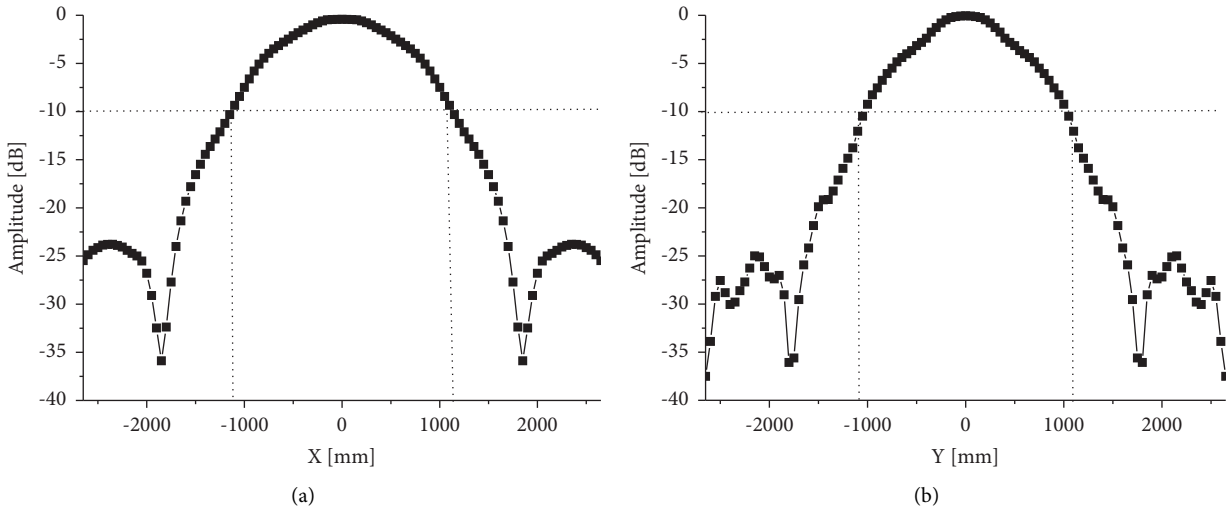

Figure 5: The computed amplitude distribution at center row and at center column. (a) The computed near field amplitude distribution at center row. (b) The computed near field amplitude distribution at center column.

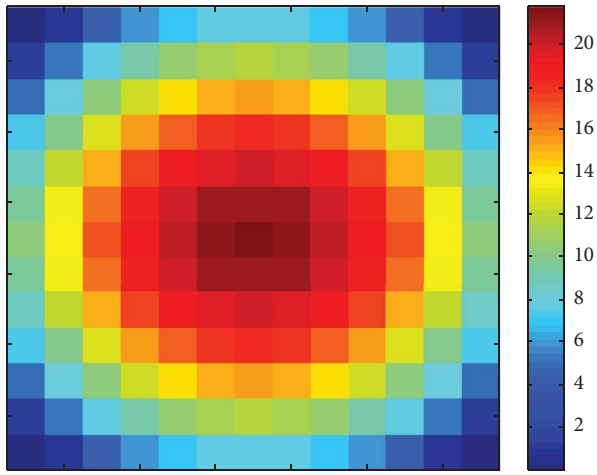

Figure 6: Received power (Pr) by the antenna element.

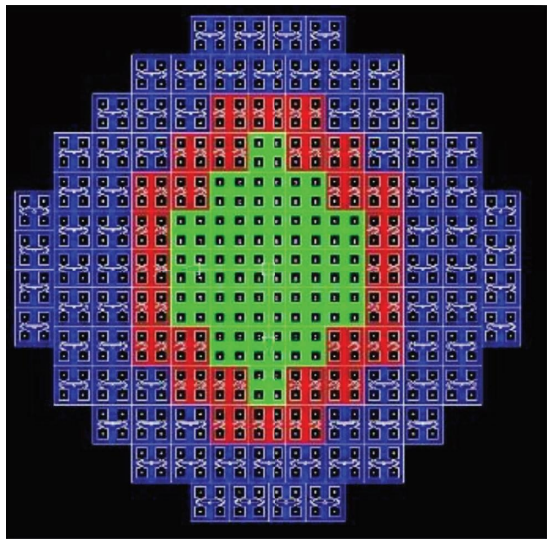

Figure 7: Schematic view of the antenna placement.

primary importance in the rectifying circuit design, and its inaccurate model would lead to a deviation of measurements from simulated results.

Figure 8 shows schematic and photographs of the diode measurement setup, which include straight calibration, reflection calibration, transmission calibration, and diode measurement circuit. The diode parameters can be obtained using the method introduced in Ref. [19]. Measured junction current I_j and junction capacitance C_j were fitted according to this model. The best fit curves and the measured data are shown in Figure 9. The final equivalent circuit model of the HSMS-282b diode is displayed in Figure 10. Therefore, the calculated diode parameters can be imported into the ADS software for the rectifying circuit design.

According to the received power analysis reported in Section 2.4, the input power to the rectifying circuit is approximately between 20 dBm and 22.6 dBm. Therefore, the expected input power to the rectifying circuit is around 21 dBm. The conversion efficiency of the rectifying circuit (η_r) is defined as

$$\eta_r = \frac{V_{DC}^2}{P_{in} R_L} \times 100\%. \tag{14}$$

The detailed design has been presented in the previous article [17]. Figure 11 shows the final rectifying circuit.

2.6. DC Combiner Circuit Design. In order to improve the power transfer efficiency, the receiver must collect as much wireless power as possible from the transmitter. The conventional method consists in RF-power combing by means of a power divider, but this technique results effective on condition that the RF power waves follow into the power divider in-phase condition. However, in the Fresnel region the received phase of the power changes at each point of the receiver because of the different path lengths from the transmitter to the receiver. Indeed, a DC combiner circuit must be designed if there is more than one rectifying circuit.

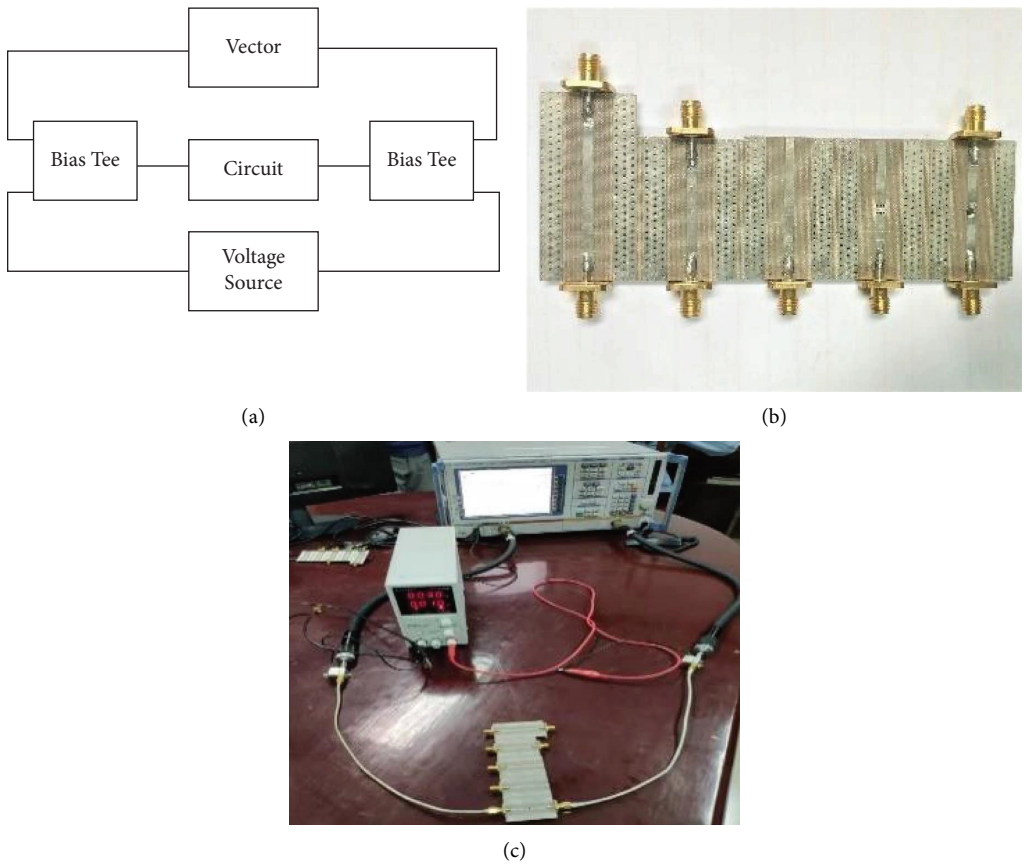

Figure 8: Schematic diagram and photographs of the diode measurement setup. (a) Schematic diagram. (b) Test circuit. (c) Photo of the test bench.

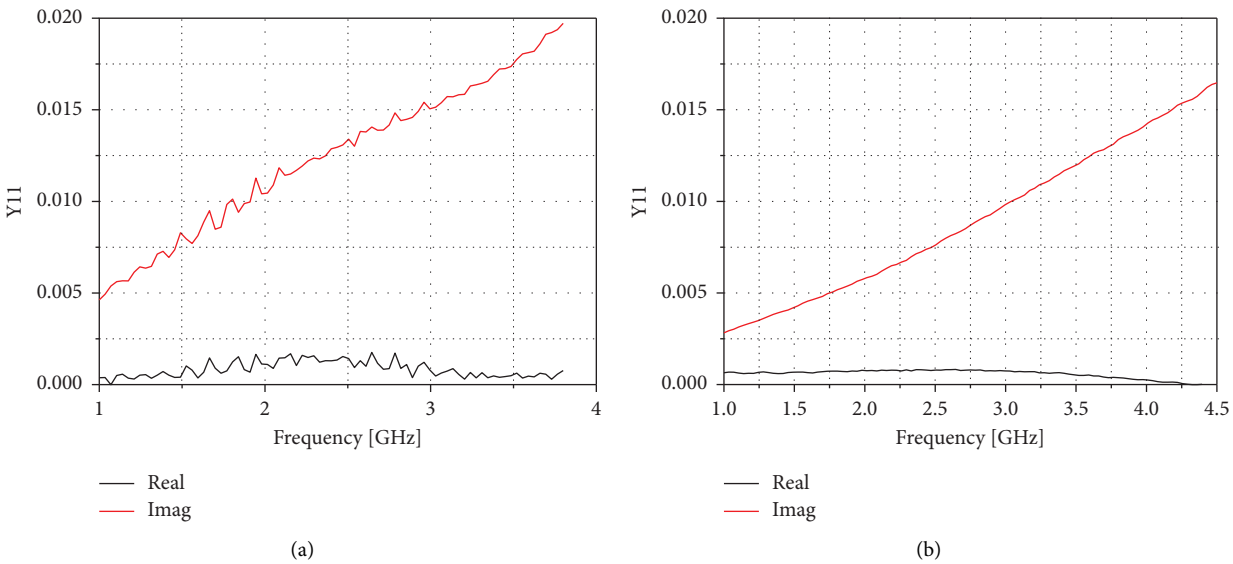

Figure 9: Continued.

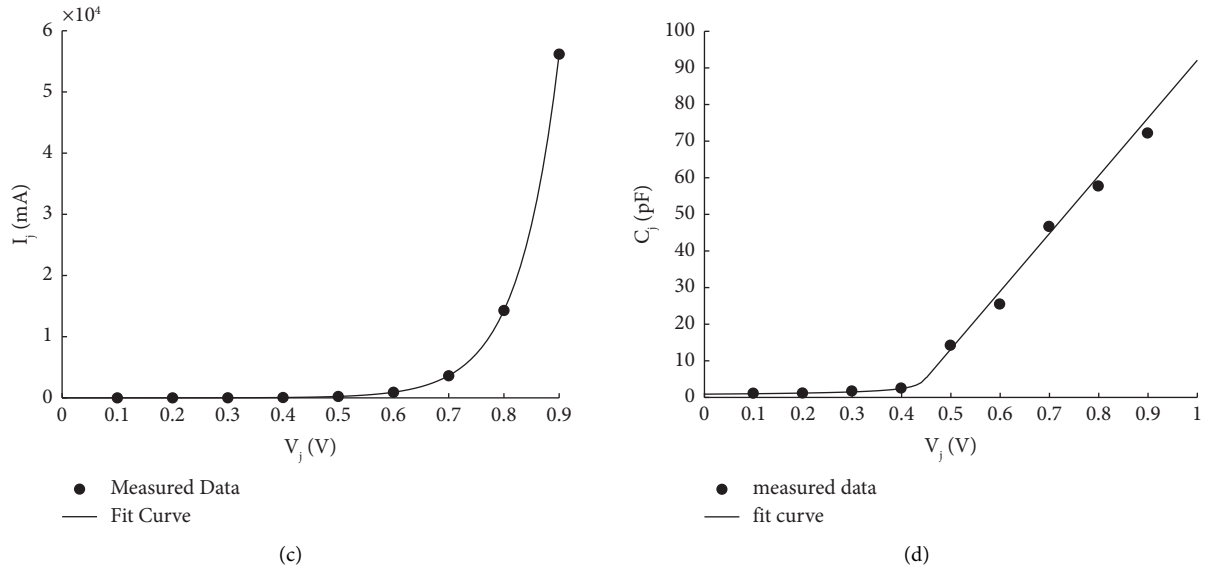

Figure 9: Results from diode measurements and fitting procedure. (a) Y-parameters of remaining voltage-dependent components when when bias voltage is −0.4 V. (b) Y-parameters of remaining voltage-dependent components bias voltage is 0.1 V. (c) Measured I_j as a function of applied voltage and best fit curve of measured data. (d) Measured C_j as a function of applied voltage and best fit curve of measured data.

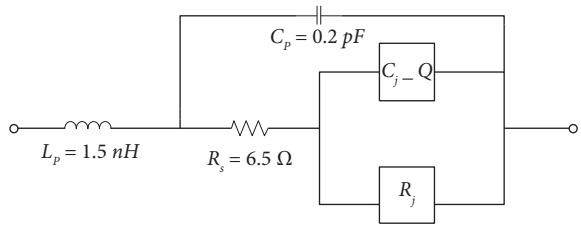

Figure 10: The final equivalent circuit model of HSMS-282b diode.

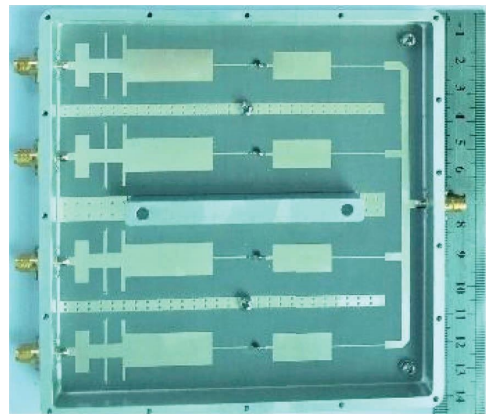

Figure 11: Photograph of the DC combiner circuit comprising four parallel rectifier circuits.

The value of the rectifying circuit load must be optimized since it will affect the overall conversion efficiency. Assuming that the load value is R when the conversion efficiency of a single rectifying circuit reaches the maximum, then the load value is $n \cdot R$ when n-th rectifying circuits are in series, and the load value is R/m when m-th rectifying circuits are in parallel. Therefore, the ultimately optimized load value is $n \cdot R/m$ in hybrid circuits. Figure 11 shows a photograph of the DC combiner circuit comprising four parallel rectifying circuits.

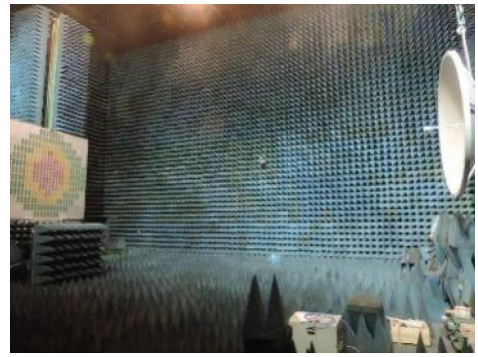

Figure 12: The designed MWPT system.

Figure 13: Back view of the receiving during testing antenna.

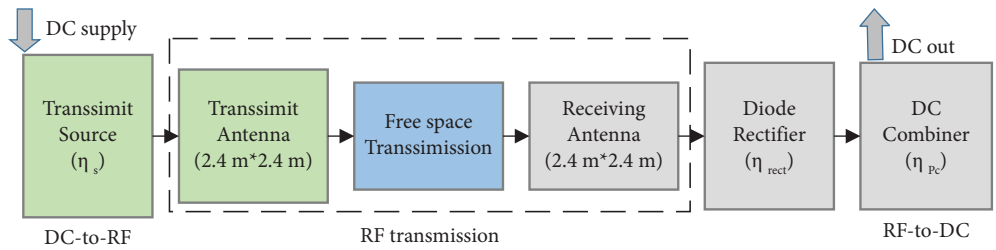

Figure 14: The efficiency configuration of the designed WPT system.

3. MWPT System Measurement

The experimental verification of the designed MWPT system is mainly aimed to illustrate the key factors which affect the WPT conversion efficiency. The WPT system is placed in an anechoic chamber, with the purpose of avoiding the electromagnetic interference. In order to reduce the transmission loss as much as possible, the connection path between the microwave transmitter and the transmitting antenna is short. Figure 12 shows a photo of the designed MWPT system during testing, the transmitting distance is 11 m. Figure 13 shows the back view of the receiving antenna. All the rectifying circuits, as well as the 214 RF ports, have been tested individually by means of a power sensor, and the total RF output power is 24.3 W.Based on the above analysis, the RF-DC conversion efficiency is strictly related to the load resistance. In the proposed design, 214 rectifying circuits are connected in parallel, so the DC load is estimated as $3500/214\,\Omega = 16.4\,\Omega$. The key factors affecting the conversion efficiency are: the DC-RF conversion efficiency (η_s), the transmission efficiency (η_{tr}), the rectifying efficiency (η_{rect}), and the DC combing efficiency (η_{pc}). Their values are 59.3%, 46.8%, 77.2%, and 90%, respectively, according to the measurement results. Figure 14 shows the efficiency configuration of the designed WPT system, and the overall conversion efficiency can be obtained by (15) based on the efficiency of each component:

$$\eta = \eta_s \cdot \eta_{tr} \cdot \eta_{rect} \cdot \eta_{pc} = 59.3\% \cdot 46.8\% \cdot 77.2\% \cdot 90\% = 20\%. \quad (15)$$

During measurements, the influence of the DC load on the overall conversion efficiency has been investigated, and the results are shown in Figure 15. The plot indicates that the maximum efficiency can reach 20% when the DC load is $16\,\Omega$. In this condition, the measured DC output voltage is

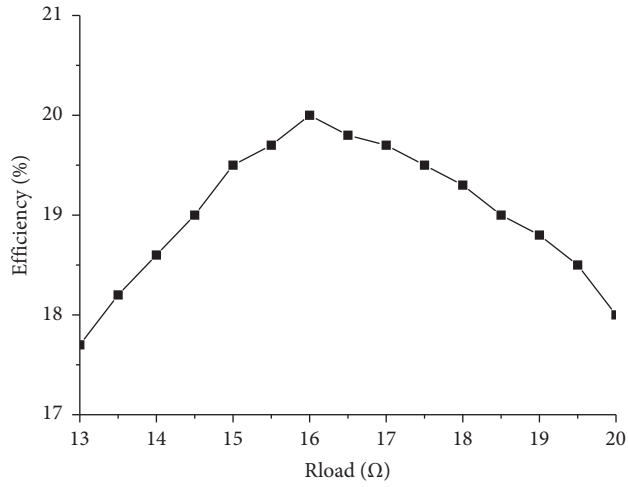

Figure 15: The DC-to-DC conversion efficiency as a function of the load resistance.

Table 2: Comparison of the proposed MWPT design with other designs reported in literature.

Ref. no	Frequency (GHz)	Polarization	Distance	RF-DC efficiency (%)	DC-DC efficiency
[9]	5.8	Circular	0.55 m	66.5	Not given
[10]	5.8	Linear	10λ	33.2	Not given
[11]	2.45	Linear	1 m	5.01	Not given
[15]	5.8	Insensitive	0.8 m	66	Not given
[16]	5.8	Circular	1 m	76.5	Not given
This work	2.45	Linear	11 m	77.2	20%

16.6 V. Table 2 summarizes the conversion efficiency achieved in the present work with that by other reported designs. The results show that the measured RF-DC and DC-DC conversion efficiencies can reach 37.5% and 20%, respectively, at a given distance of 11 m. The RF-DC conversion efficiency is higher than that reported in References [10, 11]; lower than that reported in Reference [9], but in that work the transmission distance was only 1 m. Furthermore, the mentioned references do not give the DC-DC conversion efficiency.

4. Conclusion

This paper presents the theoretical design and the experimental verification of a high-efficiency MWPT system operating in the Fresnel zone. The design principle and the corresponding equations are elaborated in detail. Finally, the MWPT system is tested in an anechoic chamber, and the total DC-DC conversion efficiency can reach 20% at a distance of 11 m. The proposed method can be useful for the applications of high-efficiency, high-power, medium-distance MWPT system operating in the Fresnel region.

Data Availability

No underlying data were collected or produced in this study.

Conflicts of Interest

The authors declare that they have no conflicts of interest.

Acknowledgments

This work was supported by the Pre-Research Project of Civil Aerospace Technology of China (D040202).

References

[1] N. Shinohara, "Power without wires," *IEEE Microwave Magazine*, vol. 12, no. 7, pp. S64–S73, 2011.

[2] P. H. Heieh, C. H. Chou, and T. Chiang, "An RF energy harvester with 44.1% PCE at input available power of-12 dBm," *IEEE Transactions on Circuits and Systems I: Regular Papers*, vol. 62, no. 6, pp. 1528–1537, 2015.

[3] L. Summerer and O. Purcell, *Concepts for Wireless Energy Transmission via Laser*, European Space Agency, Paris, France, 2008.

[4] A. P. Sample, D. A. Meyer, and J. R. Smith, "Analysis, experimental results, and range adaptation of magnetically coupled resonators for wireless power transfer," *IEEE Transactions on Industrial Electronics*, vol. 58, no. 2, pp. 544–554, 2011.

[5] M. Bogosanovic and A. G. Williamson, "Microstrip antenna array with a beam focused in the near-field zone for application in noncontact microwave industrial inspection," *IEEE Transactions on Instrumentation and Measurement*, vol. 56, no. 6, pp. 2186–2195, 2007.

[6] G. Lipworth, J. Ensworth, K. Seetharam et al., "Magnetic metamaterial superlens for increased range wireless power transfer," *Scientific Reports*, vol. 4, no. 1, pp. 3642–3646, 2014.

[7] X. Wang, B. Ruan, and M. Lu, "Retro-directive beamforming versus retroreflective beamforming with applications in

wireless power transmission," *Progress in Electromagnetics Research*, vol. 157, pp. 79–91, 2016.

[8] V. R. Garmash, B. Katsenelenbaum, S. Shaposhnikov, V. Tioulpakov, and R. Vaganov, "Some peculiarities of the wave beams in wireless power transmission," *IEEE Aerospace and Electronic Systems Magazine*, vol. 13, no. 10, pp. 39–41, 1998.

[9] Y. Z. Dong, S. W. Dong, Y. Wang et al., "Focused microwave power transmission system with high-efficiency rectifying surface," *IET Microwaves, Antennas and Propagation*, vol. 12, no. 5, pp. 808–813, 2018.

[10] V. R. Gowda, O. Yurduseven, G. Lipworth, T. Zupan, M. S. Reynolds, and D. R. Smith, "Wireless power transfer in the radiative near field," *IEEE Antennas and Wireless Propagation Letters*, vol. 15, pp. 1865–1868, 2016.

[11] S. T. Khang, D. J. Lee, I. J. Hwang, T. D. Yeo, and J. W. Yu, "Microwave power transfer with optimal number of rectenna arrays for midrange applications," *IEEE Antennas and Wireless Propagation Letters*, vol. 17, no. 1, pp. 155–159, 2018.

[12] X. Li, K. M. Luk, and B. Y. Duan, "Aperture illumination designs for microwave wireless power transmission with constraints on edge tapers using bezier curves," *IEEE Transactions on Antennas and Propagation*, vol. 67, no. 2, pp. 1380–1385, 2019.

[13] R. T. Farouki, "The Bernstein polynomial basis: a centennial retrospective," *Computer Aided Geometric Design*, vol. 29, no. 6, pp. 379–419, 2012.

[14] X. Li, B. Duan, J. Zhou, L. Song, and Y. Zhang, "Planar array synthesis for optimal microwave power transmission with multiple constraints," *IEEE Antennas and Wireless Propagation Letters*, vol. 16, pp. 70–73, 2017.

[15] M. Y. Chang, Y. C. Li, J. Q. Han, H. X. Liu, and L. Li, "A compact polarization-insensitive rectenna with harmonic suppression for wireless power transfer," *IEEE Antennas and Wireless Propagation Letters*, vol. 23, no. 1, pp. 119–123, 2024.

[16] C. F. Cao, X. M. Zhang, C. Y. Song, A. Georgiadis, and G. Goussetis, "A highly integrated multipolarization wideband rectenna for simultaneous wireless information and power transfer (SWIPT)," *IEEE Transactions on Antennas and Propagation*, vol. 71, no. 10, pp. 7980–7991, 2023.

[17] X. Li, L. Yang, and L. Huang, "Novel design of 2.45-GHz rectenna element and array for wireless power transmission," *IEEE Access*, vol. 7, no. 1, Article ID 28356, 2019.

[18] X. Y. Zhang, Z. X. Du, and Q. Xue, "High-efficiency broadband rectifier with wide ranges of input power and output load based on branch-line coupler," *IEEE Transactions on Circuits and Systems I: Regular Papers*, vol. 64, no. 3, pp. 731–739, 2017.

[19] M. He, H. C. Sun, Z. Zhong, Y. X. Guo, and M. Y. Xia, "Technology-independent table-based diode model for rectenna design in RF energy harvesting," in *Proceedings of the 2012 IEEE International Symposium on Antennas and Propagation*, pp. 1-2, Chicago, IL, USA, July 2012.